ADVANCED MATERIALS
www.advmat.de

Ultraviolet Light Debondable Optically Clear Adhesives for Flexible Displays through Efficient Visible-Light Curing

Daewhan Kim, Hongdeok Kim, Woojin Jeon, Hyun-Joong Kim, Joonmyung Choi, Youngdo Kim,* and Min Sang Kwon**

With growing sustainability concerns, the need for products that facilitate easy disassembly and reuse has increased. Adhesives, initially designed for bonding, now face demands for selective removal, enabling rapid assembly-disassembly and efficient maintenance across industries. This need is particularly evident in the display industry, with the rise of foldable devices necessitating specialized adhesives. A novel optically clear adhesive (OCA) is presented for foldable display, featuring a unique UV-stimulated selective removal feature. This approach incorporates benzophenone derivatives into the polymer network, facilitating rapid debonding under UV irradiation. A key feature of this method is the adept use of visible-light-driven radical polymerization for OCA film fabrication. This method shows remarkable compatibility with various monomers and exhibits orthogonal reactivity to benzophenone, rendering it ideal for large-scale production. The resultant OCA not only has high transparency and balanced elasticity, along with excellent resistance to repeated folding, but it also exhibits significantly reduced adhesion when exposed to UV irradiation. By merging this customized formulation with strategically integrated UV-responsive elements, an effective solution is offered that enhances manufacturing efficiency and product reliability in the rapidly evolving field of sustainable electronics and displays. This research additionally contributes to eco-friendly device fabrication, aligning with emerging technology demands.

1. Introduction

With sustainability gaining more significance in modern society,[1] it is imperative that product design emphasizes easy disassembly for reuse and recycling.[2] In this context, adhesives should not only perform their primary function of bonding materials but also possess the ability for selective removal when necessary.[3] Various methods for the selective removal of adhesion have been proposed, including thermal,[4,5] magnetic,[6] electric,[7] chemical,[8,9] pH-responsive,[10] metal-ion based,[11] and photocuring techniques.[12,13] Such debondable adhesives can be efficiently employed not just for reuse or recycling purposes but also for quick assembly-disassembly processes, as well as for repairing and upgrading components across multiple industries.[14,15]

The smartphone, an essential display device in our daily lives, owes its versatility and durability to the integration of distinct components, each performing designated functions, bound together by adhesives. With the emergence of devices showcasing diverse form factors,[16] such as foldable phones, the demand for multifunctional adhesives has risen. Hence, adhesives must not only bond individual element films but also offer stress-dissipation properties with an optimal balance of flexibility and elasticity,[17] provide optical transparency and clarity,[18] ensure high moisture, and possess heat resistance,[19] and in some cases, even possess UV light blocking capabilities.[20] However, the growth of diverse form factors has complicated electronic device structures, occasionally leading to film lamination failures (**Figure 1a**). These failures can be especially burdensome when high-cost components like display panels and

D. Kim, W. Jeon, M. S. Kwon
Department of Materials Science and Engineering
Seoul National University
Seoul 08826, Republic of Korea
E-mail: minsang@snu.ac.kr

H. Kim, J. Choi
Department of Mechanical Design Engineering
Hanyang University
Seoul 04763, Republic of Korea
E-mail: joonchoi@hanyang.ac.kr

The ORCID identification number(s) for the author(s) of this article can be found under https://doi.org/10.1002/adma.202309891

DOI: 10.1002/adma.202309891

H. Kim, J. Choi
Department of Mechanical Engineering
BK21 FOUR ERICA-ACE Center
Hanyang University
Ansan 15588, Republic of Korea

H.-J. Kim
Department of Agriculture
Forestry and Bioresources
Seoul National University
Seoul 08826, Republic of Korea

Y. Kim
Mobile Display Module Development Team
Samsung Display Co., Ltd.
Cheonan 31086, Republic of Korea
E-mail: colour.kim@samsung.com

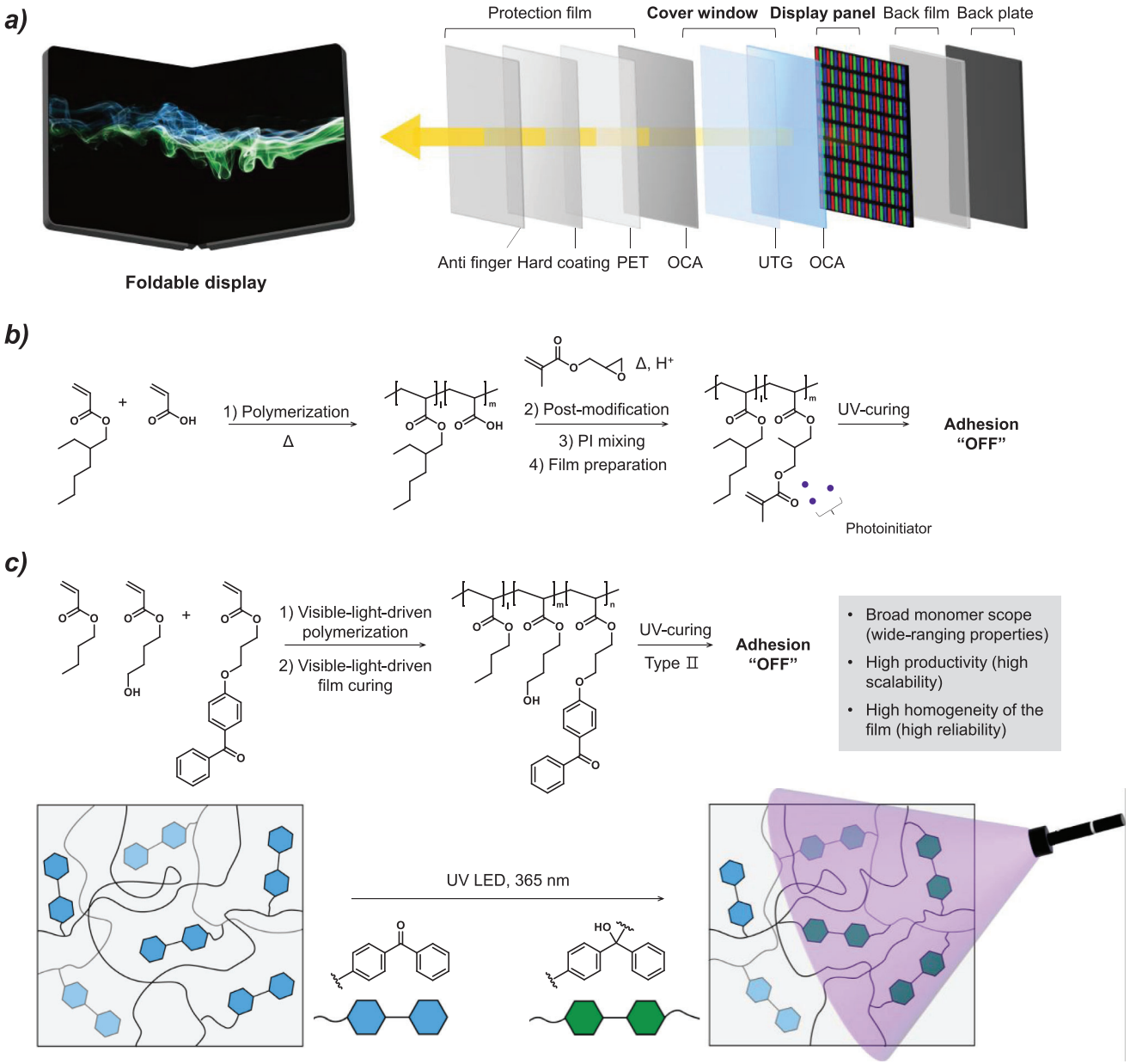

Figure 1. a) Structure of the foldable display, showcasing the optically clear adhesive (OCA) that binds the ultrathin glass (UTG) to the display panel. b) The conventional UV-debondable adhesive is produced with an acrylic moiety as a pendant group from a backbone, necessitating both solvent and heat for its formation. c) Proposed method of curing the UV-debondable adhesive using visible-light-driven polymerization (top) and conceptual illustration of the UV-debondable adhesive being cured under visible light, depicting the crosslinking from initial BP (blue) to the responsive BP (green) under UV irradiation (bottom).

ultrathin glass (UTG) are implicated, thereby escalating manufacturing expenses.[21] Notably, lamination failures in larger displays, such as tablet computers, can drastically inflate production costs. To minimize costs, it is vital to detach the adhesive from expensive components to facilitate their reuse. Yet, this procedure can be intricate and potentially damage the components. For instance, removing the adhesive layer from foldable smartphone displays necessitates elevated temperatures, specialized machinery, and further chemical cleaning to remove remaining residues (Figure S22, Supporting Information (SI)). An adhesive that fulfills all the requisites for foldable smartphone applications, while being effortlessly detachable via external stimuli, would be the optimal solution to the challenges of adhesive removal and device reusability. Unfortunately, as of now, such an adhesive remains underdeveloped and unavailable in the market. Ideally, the adhesive should be producible using the existing photocuring method.

Here, we introduce an optically clear adhesive (OCA) specifically designed for foldable smartphones, which not only satisfies all the essential criteria for OCA application in such devices

but also boasts a unique ability for selective removal through UV stimulation. Our approach to achieving rapid on-demand debonding involves incorporating benzophenone derivatives into the polymer network. This promotes additional crosslinking through UV-induced Norrish type II reactions, leading to debonding at the adhesive-substrate interface.[22] A key aspect of our approach is the utilization of visible-light-driven radical polymerization for the fabrication of the OCA films. This technique demonstrates orthogonal reactivity with benzophenone and offers excellent compatibility with a range of monomers, making it highly suitable for large-scale production. The OCA film derived from this approach, using an appropriate blend of acrylic monomers with 3 mol% of benzophenone-derived acrylates, delivered remarkable results. This formulation resulted in a drastic reduction in adhesion (from 2.44 to 0.14 N·cm^{-1}) when exposed to the suitable UV irradiation dosage (4200 mJ cm^{-2}), enabling facile removal of the adhesive from both UTG and display panels without any residual traces. In addition, the prepared OCA film exhibited high optical transparency (>99%) and commendable peel strength (2.76 N cm^{-1}). It maintained a balance between stress relaxation and strain recovery, and also demonstrated remarkable folding durability, showing no defects even after rigorous dynamic folding tests under varied conditions (25, −20, and 60 °C with 93% humidity), nearly satisfying the standards for commercial foldable displays.

2. Results and Discussion

2.1. Strategy

Utilizing photoinduced overcuring stands as a key strategy for achieving photodebondable adhesives.[23] Although the molecular mechanism is not entirely elucidated, it is well-established that volume shrinkage resulting from overcuring is the primary factor.[24] This strategy primarily employs UV-sensitive polymer blends that incorporate a photoinitiator activated by UV light, in combination with polymers featuring acrylic moieties as pendent groups (Figure 1b). These methods typically involve solvent-based polymerization and post-polymerization modification, necessitating additional processing time and leading to the emission of volatile organic compounds.[25,26] The process comprises at least four steps: i) Free radical polymerization, ii) post-polymerization modification, iii) blending with a photoinitiator, and iv) film preparation. Specifically, the post-polymerization modification requires the incorporation of certain monomers (e.g., acrylic acid, maleic anhydride, etc.) into the polymer, which subsequently restricts the range of physical properties achievable in the final adhesive. This limitation poses a challenge for foldable OCAs.

To tackle this issue, we utilized solvent-free visible-light-driven radical copolymerization to prepare the OCA film. Note that visible-light-driven polymerization, which relies on the effective absorption of visible light by a photosensitizer, has been applied in diverse applications[20,27–29] due to its numerous advantages over traditional UV light including higher energy efficiency, safety for humans, and fewer side reactions.[30–35] In the current study, we established a photoinitiating system (PIS) comprised of a cyanoarene molecule as a photocatalyst (PC) and tertiary amines as co-initiators (**Figure 2a**). Cyanoarene PCs usually exhibit long-lived triplet excited states,[36–38] facilitating photocuring with minimal PC amounts and ensuring superior optical transparency within the visible light spectrum.[20,39] Moreover, we incorporated an acrylic monomer substituted with benzophenone as an essential ingredient. This specific component shows negligible reactivity towards both visible light and active radical species; however, it does facilitate the generation of additional crosslinking via UV-induced reactions.[40–43] As a result, our approach enables the efficient two-step production of the OCA film, designed to have significantly reduced adhesion under UV exposure, aligning with the established commercial OCA film production method of two-step photocuring: i) Visible-light-driven polymerization to prepare acrylic syrup and ii) visible-light curing to prepare the film.[43–45] Given the high efficiency of the Norrish type II reaction involving benzophenone, only a minimal amount of the benzophenone monomer is necessary.[46] This enables the utilization of a diverse range of monomers, optimizing adhesion and viscoelastic properties in the OCA. A full description of the synthesis and characterization of the benzophenone-based monomer (3-(4-benzoylphenoxy)propyl 2-propenoate, denoted as BP, as well as the PC including ^{1}H/^{13}C NMR spectra and high-resolution mass spectra, is available in the SI.

2.2. Preparation of UV-Debondable OCAs

Figure 2a illustrates the process of producing a UV-debondable OCA film. Similar to conventional acrylic OCAs, this method involves the bulk polymerization of acrylic monomers, followed by photoinduced film curing. For this study, n-butyl acrylate (BA) and 4-hydroxybutyl acrylate (HBA) were selected as monomers. Their suitability in creating OCAs designed for foldable displays has been documented previously.[20] BA, with its low glass transition temperature (T_g), provides excellent flexibility to OCAs, even at low temperatures. HBA is incorporated to improve the cohesive strength of OCAs. We utilized 452 nm LEDs as the light source, 4Cz-IPN as the PC, and a combination of two tertiary amines (i.e., dimethylaminoethyl acrylate (DMAEA) and dimethylaminoethyl acetate (DMAEAc)) as co-initiators.[20] 4Cz-IPN takes advantage of excited triplet states for electron transfer, allowing for rapid curing even with a minimal PC concentration (10 ppm). This leads to an OCA film with highly transparent in the visible-light spectrum. Tertiary amines function both as initiators, forming α-amino radicals through electron transfer with 4Cz-IPN (Figure 2a, mechanism), and oxygen scavengers.[47,48] Furthermore, DMAEA serves as a crosslinker, enhancing the gel content to ensure that the OCA maintains proper cohesion.[20] In order for benzophenone to exhibit orthogonal reactivity in this selected PIS, it is essential that benzophenone does not absorb the excitation light. Additionally, interactions such as electron or energy transfer between 4Cz-IPN and the BP monomer must be minimized. To confirm this, we obtained the Stern–Volmer relationship through the emission quenching of 4Cz-IPN (Figure S9a, Supporting Information). Interestingly, noticeable emission quenching was observed in the presence of the benzophenone monomer, leading us to derive a quenching constant (k_q) of 2.3×10^6 M^{-1}•s^{-1}. To better understand the photophysical processes behind this emission quenching, we determined the redox

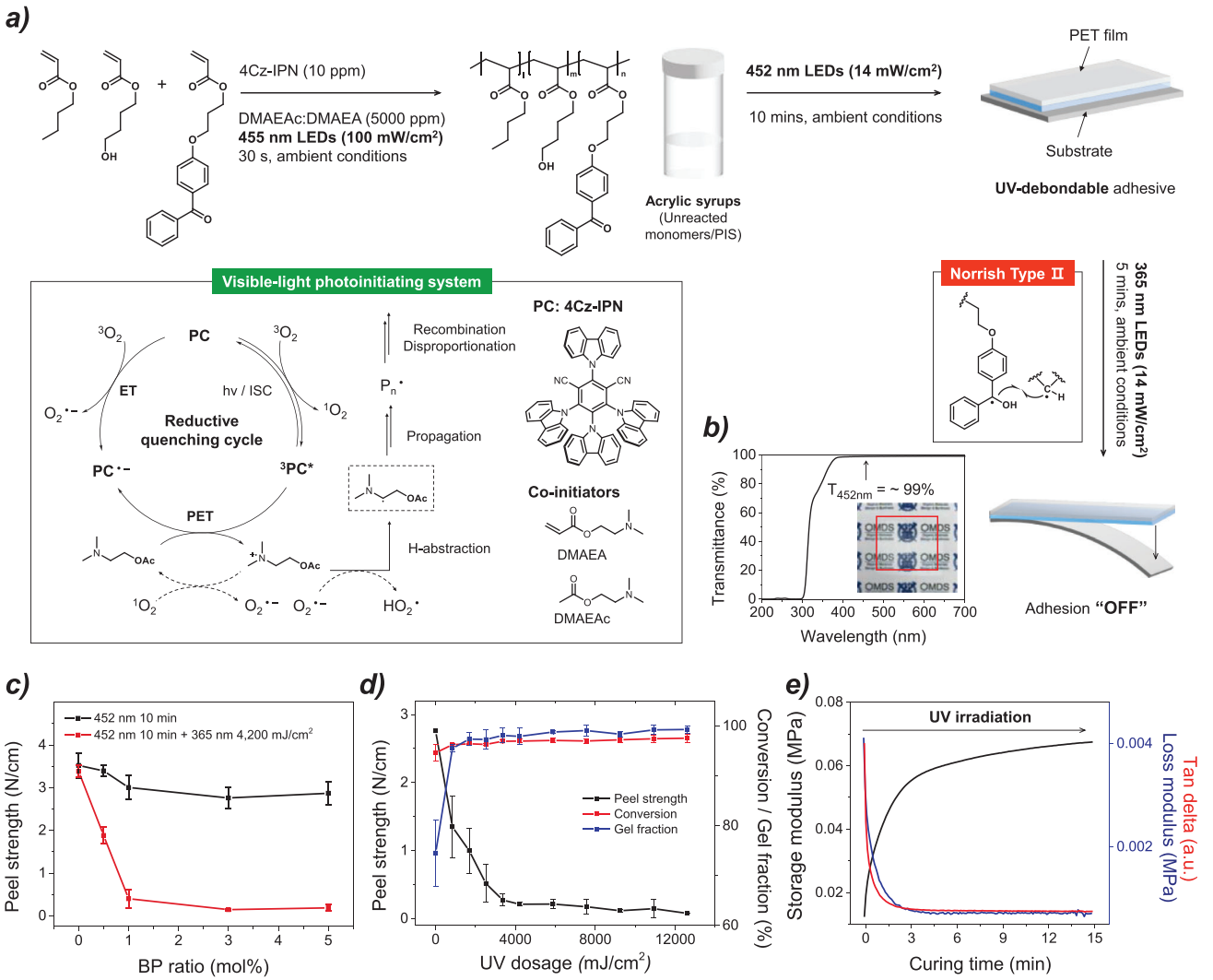

Figure 2. a) Strategies and mechanisms for photocuring a UV-debondable adhesive using visible light, and for the selective removal of adhesion through UV irradiation. b) Optical properties of UV-debondable adhesive, demonstrating ≈99% transmittance and confirming visual transparency. c) Comparison of peel strength reduction in UV-debondable adhesive after UV irradiation, based on varying BP content. d) Evaluation of peel strength, conversion, and gel fraction changes in UV-debondable adhesive with 3 mol% BP content in relation to different UV dosages. e) Rheometer measurements employed to assess the viscoelastic properties during the simultaneous UV curing of the adhesive.

potential, the frontier molecular orbital energies, and the triplet energies of both 4Cz-IPN and the BP monomer (Figure S9b–g, Supporting Information). These assessments were made through experimental methods and quantum chemical calculations. Based on these data, we propose that electron transfer from BP to 4Cz-IPN is the primary quenching mechanism. Although this electron transfer from BP to 4Cz-IPN occurs at a fairly high rate, particularly when compared to the electron transfer rate between 4Cz-IPN and tertiary amines (DMAEA and DMAEAc; $k_q = 2.1 \times 10^7$ $M^{-1}•s^{-1}$), the benzophenone functional group remains unreacted and well-preserved during polymerization under 455 nm LED irradiation (see below; for detailed discussions, see Table S3, Supporting Information). We assume the preservation of the benzophenone functional group is due to its immediate reduction by tertiary amines. Following the formation of a radical cation through electron transfer with 4Cz-IPN, the benzophenone moiety is rapidly reduced by the amines, reverting to its original state. As a result, it may not significantly impact the overall catalytic reaction process. All experiments were conducted in ambient conditions without the need for inert gas sparging. The optimal components for foldable OCAs are as follows: A mixed ratio of eight parts BA to two parts HBA by volume; amine co-initiators DMAEAc and DMAEA with a total concentration of 5000 ppm with a mole ratio of 6:4, respectively; varying amounts of BP; and 10 ppm mole amount of 4Cz-IPN relative to the total monomer. Using these parameters, we prepared five distinct films by adjusting the BP quantities (0, 0.5, 1, 3, and 5 mol% BP, respectively). It is worth noting that the OCA films have a 50 μm thickness and were manufactured using a conventional 50 μm-thick poly(ethylene terephthalate) film (PET_f) paired with an attached release film (silicone-treated 100 μm-thick PET_f).

2.3. Properties of UV-Debondable OCAs

Excellent visible-light transmittance was observed in all five films as shown in Figure 2b. Although there was a slight decrease in adhesion as the BP content increased, all films demonstrated adequate peel strength suitable for OCA applications in foldable displays. Following this, adhesion reduction experiments were performed by exposing the five films to additional UV light. The exposure was set at ≈4200 mJ cm^{-2}, a level deemed appropriate to prevent damage to the underlying display panel of the device.[49] For the OCA film without any BP, UV exposure did not lead to any decrease in adhesion. However, in line with expectations, the four films containing BP showed a notable decrease in adhesion, as seen in Figure 2c. The decline in adhesion was proportional to the BP content. Importantly, the OCA film with 3 mol% BP showed an ≈10-fold reduction in adhesion, positioning it as a prime candidate for a UV-debondable OCA given its dramatically reduced post-curing adhesion. In contrast, the film with 0.5 mol% BP experienced only a 55% drop in adhesion, even when exposed to higher light levels of around 12 600 mJ cm^{-2}. This might be due to insufficient post-crosslinking among polymers, likely resulting from an inadequate overall BP quantity. Intriguingly, even when BP content exceeded 3 mol% and peaking at 5 mol%, no further reduction in adhesion was noted. Overall, these results suggest that UV light-induced post-crosslinking of BP groups directly influences the polymer network, leading to a decrease in adhesion.

To thoroughly understand the mechanism underlying the decrease in adhesion, we studied changes in monomer conversion, gel fraction, and adhesion in relation to the UV dose (Figure 2d). For this study, we focused on an OCA film containing 3 mol% BP, given its optimal peel strength and UV-debondable properties. As expected, due to the thorough curing of the OCA during its production which minimized unreacted monomer, there was negligible change in monomer conversion as the UV dose increased. In contrast, the gel fraction rose with increasing cumulative UV irradiation. It is worth noting that OCA films designed for foldable displays typically target a gel fraction of around 70% within an optimal monomer composition. This strikes the right balance between flexibility and elasticity. After an initial UV dose of 840 mJ cm^{-2}, the gel fraction jumped from ≈70% to 90%. Thereafter, it continued to rise until it reached a UV dose of around 4000 mJ cm^{-2}, where it plateaued. This observed behavior can be ascribed to the continuous post-crosslinking of polymer chains mediated by the BP moieties situated in the pendants of the polymer chains during UV exposure. A significant correlation was noted between the rising gel fraction and the consistent decrease in peel strength. Rheometer tests were conducted with UV irradiation simultaneously, providing insight into the UV-induced debonding mechanism. As the UV irradiation increased, the storage modulus showed a continuous uptrend, mainly due to the enhanced crosslinking between polymer chains mediated by BP (Figure 2e). The notable rise in the storage modulus signifies a prominent increase in the adhesive's elasticity. This increased cohesiveness of the adhesive likely serves a dual role: i) Initiating volume shrinkage within the OCA and ii) ensuring efficient transmission of external forces to both the adhesive and substrate surfaces. This intricate interplay is presumably the driving force behind the observed reduction in peel strength.

2.4. Origin of Debonding Behavior

The phenomenon wherein debonding occurs due to UV irradiation is widely acknowledged. It is primarily attributed to a reduction in the adhesive's bonding surface area, caused by overcuring-induced shrinkage.[23] This decreased surface area results in reduced wetting of the substrate, culminating in debonding at the adhesive–substrate interface. Beyond the adhesive's wetting behavior, the rheological characteristics of the polymers are instrumental in determining their adhesion performance, as previously hypothesized. To provide a theoretical perspective on the contribution of the photochemical reaction of benzophenone in interfacial bonding, we conducted all-atom molecular dynamics (MD) simulations. Detailed descriptions of the modeling procedure and simulation environment can be found in the Supporting Information.

We constructed two model systems of acrylic adhesive/SiO_2 bilayers: One representing the state before UV irradiation and the other after UV exposure. These systems imitate experimentally derived OCAs, incorporating a blend of polymer networks and residual monomers onto the amorphous SiO_2 surface. The monomer conversion of the acrylic adhesive, prior to UV irradiation, was determined to be 91.5%, which aligns closely with the experimental value of 96.2%. The microstructure of the adhesive, following UV irradiation, was modeled to account for the increased crosslinking caused by UV exposure to benzophenone, as illustrated in **Figure 3**a. The photochemical reaction of benzophenone resulted in a significant alternation of the topological features of the OCA network. In particular, numerous dangling chains within the adhesive network experienced crosslinking following UV exposure (Figure 3b). As a result, there was a notable increase in the internal connectivity, or cohesion, of the OCA network, which aligns well with the rheological results shown in Figure 2e.

This improvement in connectivity was evident in the adhesive behavior observed during the delamination simulation at the acrylic adhesive/SiO_2 interface (Figure 3c, bottom). The stress profiles of the SiO_2 substrate, when compared during the delamination simulations for both models, showed a marked difference. It is important to note that the stress mentioned here differs from the stress applied to the OCA, and for additional clarity, Figure S25, Supporting Information illustrates the stress-strain curve of the OCA as predicted by simulation. The non-irradiated OCA requires more displacement for fracture initiation, whereas the UV-treated adhesive needs less displacement to begin fracturing. This indicates that the adhesion of pre-irradiated OCA is stronger, necessitating greater force during debonding, a finding consistent with the experimental results shown in Figure 3c, top.

The difference in mechanical behavior becomes more pronounced when observing the distribution of von Mises strain (ϵ_e) experienced by the OCA network at each significant stage of the stress-displacement profile, as depicted in Figures 3d,e. For the acrylic adhesive prior to UV irradiation, the deformation process involves the following sequential steps: i) The stress in the SiO_2 substrate rises linearly until the yield point, indicating the onset of cavitation in the polymer network, ii) as cavities within the OCA network continue to expand, there is a decrease in the load transferred by the OCA chain to the interface, keeping the stress on the SiO_2 substrate below the yield point, iii) the OCA

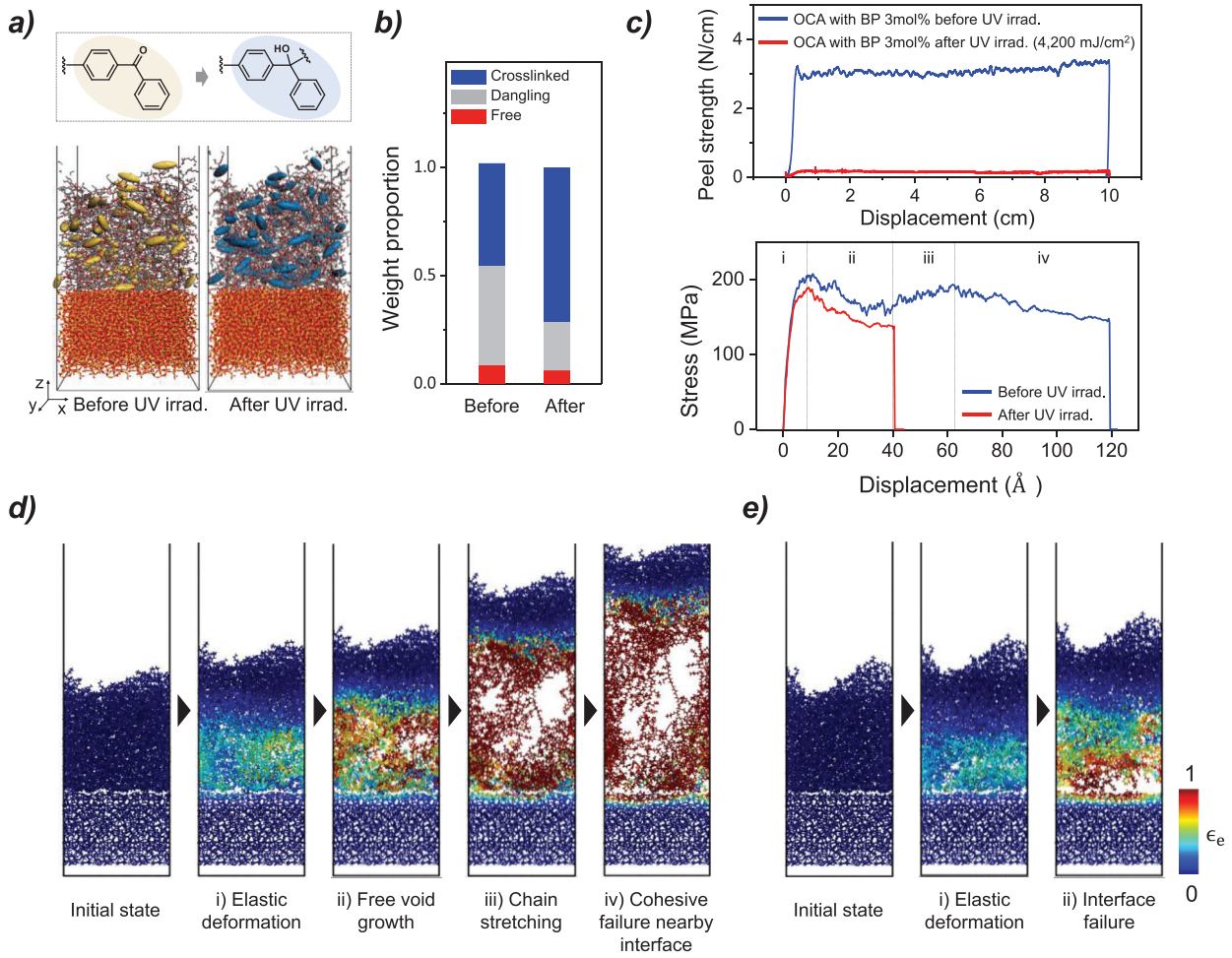

Figure 3. Mechanistic understanding of the change in adhesion performance due to the photochemical reaction of BP, as depicted by all-atom MD simulations. a) Molecular configurations of OCA/SiO_2 showcasing unreacted (yellow) and reacted BP (blue). Hydrogen atoms have been omitted for clarity. b) Weight fraction representations of the free state, dangling state, and crosslinked state backbones of the OCA network. c) Comparative analysis of adhesive strength before and after photochemical reaction: experimental peel strength measurements (top) and MD simulations of stress profile on the SiO_2 substrate (bottom). d) Representative images showing the delamination of OCA networks from SiO_2 substrates prior to UV irradiation. e) Illustration of OCA delamination post-UV irradiation, with atoms colored based on the magnitude of the von Mises strain (ϵ_e) experienced.

network undergoes fibrillation, prompting the molecular chains inside the cavities to tighten, and iv) failure occurs when the OCA chains to the SiO_2 surface detach completely from the bulk region, leaving a myriad of residues behind.

In contrast, the deformation process of the UV-irradiated OCA's is notably simplified. The network exhibits elastic behavior similar to its non-irradiated counterpart but with a slightly lower yield point. While cavities in the UV-irradiated OCA appear at displacements similar to those in the non-irradiated sample, their expansion is significantly hindered due to increased chain connectivity from crosslinking. This enhanced connectivity restricts molecular mobility, leading to stress concentration at the boundary of the OCA/SiO_2 layers and resulting in failure without residue. These simulations demonstrate how additional UV-induced crosslinking dramatically enhances the OCA network's cohesion from a topological perspective, leading to stress concentration at the interface and causing premature adhesive failure without any residue. These MD simulations offer valuable insights into the causes of the changes observed experimentally in adhesive properties, intricately linked to the polymer system's topology, and align well with established debonding mechanics and fracture mechanics models of soft adhesives, for example, the Lake–Thomas theory.[50]

2.5. Properties for Foldable OCA

The successful implementation of foldable displays relies on the OCA's ability to retain its bonding properties across repeated folding cycles without alternations in its physical characteristics. In this context, the OCA should demonstrate high-stress relaxation to absorb stresses generated during folding effectively. It should also have a high strain recovery capability to revert to its original form post-deformation. To identify the ideal OCA for foldable displays, we introduced 2-ethylhexyl acrylate (EHA) and 2-hydroxyethyl acrylate (HEA) as low T_g monomers, in addition

Table 1. Summary of viscoelastic properties and adhesion of the UV-debondable OCAs with different monomer combinations. Strain recovery and stress relaxation were measured via dynamic mechanical analysis (DMA) testing at room temperature. Peel strength was assessed on four different substrate types, with changes in adhesion documented post-UV irradiation. While UV irradiation penetrated most substrates, CPI and PI films absorbed UV in the UV region, making subsequent peel strength measurements after UV irradiation impractical.

Entry	Monomer	Monomer ratio	BP ratio [%]	Strain recovery before UV at 25 °C [%]	Stress relaxation before UV at 25 °C [%]	Peel strength before [after] UV irradiation at 25 °C [N cm^{-1}]				UV dosage [mJ cm^{-2}]
						Glass	UTG	CPI	PI	
1	BA:HBA	0.8:0.2	3	67.5 (± 1.3)	62.5 (± 1.6)	2.76 [0.14]	2.45 [0.23]	7.17	6.70	4200
2	BA:HEA	0.8:0.2	3	66.2 (± 0.1)	60.7 (± 1.9)	3.84 [1.72]	2.98 [0.77]	6.34	3.21	4200
3	EHA:HBA	0.8:0.2	3	82.5 (± 2.1)	65.1 (± 4.9)	3.56 [0.26]	2.41 [0.31]	5.29	4.97	4200
4	EHA:HEA	0.8:0.2	3	72.1 (± 0.3)	56.5 (± 0.8)	4.14 [1.40]	3.30 [0.96]	4.22	4.21	4200
5	CEF 3602 (Foldable OCA)			86.1 (± 2.2)	47.5 (± 1.3)	4.8	0.97	5.78	3.34	–

to the previously used BA and HBA. We then quantitatively assessed stress relaxation and strain recovery.

DMA measurements were conducted to explore stress relaxation and strain recovery for four distinct OCAs prepared using the monomers mentioned above, prior to UV curing (**Table 1**). All formulated OCAs incorporated 3 mol% of BP to confer UV-debondable property. Among the tested combinations, the inclusion of EHA and HBA monomers exhibited a promising performance: 82.5% strain recovery and a 65.1% stress relaxation ratio (Table 1, entry 3). These results demonstrate comparable strain recovery values (86.1%) and significantly outperform the stress relaxation value (47.5%) of CEF 3602, a conventional foldable OCA developed by 3 M.

Subsequent peel strength measurements were carried out before and after UV curing for these OCAs. We employed UTG, polyimide (PI), colorless PI (CPI), commonly utilized materials in flexible displays, and conventional glass as substrates to evaluate peel strength. While all four prepared films exhibited variations in adhesive strength based on the substrate, the initial adhesion was suitable for use as foldable display OCAs across all substrates. Typically, stronger adhesion was observed on PI than on glass. In every film, UV irradiation at a dose of 4200 mJ cm^{-2} led to reduced adhesion. The extent of this reduction varied significantly depending on the polar monomer used. Films incorporating HEA as a monomer exhibited an adhesion drop of about 2–3 times (Table 1, entries 2 and 4). Conversely, those using HBA as a monomer experienced a dramatic dip in adhesive strength, around 10–30 times (Table 1, entries 1 and 3). Intriguingly, the non-polar monomers (i.e., BA and EHA) barely influenced the results. Ongoing research aims to shed light on the variable adhesive strengths attributed to the monomer type. EHA and HBA combinations, containing 3 mol% of BP, stood out when considering viscoelastic properties and UV-induced adhesion reduction tests. A dynamic folding ensued to ascertain the applicability of the UV-debondable OCA we devised for foldable displays. The details of this dynamic folding test, grounded in previous research, are thoroughly outlined in the Supporting Information.

For the dynamic folding test, we selected the combination of BA and HBA (Table 1, entry 1) and EHA and HBA (entry 3) combinations due to their outstanding viscoelasticity and mechanical properties. For comparative purposes, the CEF 3602 adhesive from 3 M, typically used for foldable OCAs, was also tested (Table 1, entry 5). Recognizing the imperative for these adhesives to function flawlessly under real climatic conditions, accelerated testing was employed. Testing was conducted with three samples exposed to stringent conditions: i) −20 °C 100 000 folding, ii) room temperature 200 000 folding, and iii) 60 °C 93% relative humidity (RH) 100 000 folding cycles. Simulating a foldable smartphone's configuration, UV-debondable OCA was positioned between PI and CPI films (**Figures** 4a and S17, Supporting Information).[51] After every 10 000 folding cycles, inspection was done to identify any crack formation and to compare the *z*-axis displacement (ΔZ) between the folded and pre-folded samples (Figures 4b and 4c).

No cracks were observed in the −20 °C, 100 000-fold test across all samples (Figure S18, Supporting Information). However, under room temperature and 60 °C 93% RH conditions, one of the three BA: HBA samples (Table 1, entry 1) displayed crack formation (Figures S19 and S20, Supporting Information). The formation of cracks at room temperature can likely be attributed to the BA:HBA combination's relatively high modulus in comparison to other films (Table S4, Supporting Information). A high storage modulus at room temperature indicates a decrease in the viscosity of the OCA, leading to increased stress and reduced stress relaxation. This culminates in wrinkle buildup and, subsequently, crack formation. On the other hand, the appearance of cracks during high-temperature, high-humidity experiments can be ascribed to the BA:HBA combination. Among the three sample combinations tested (Table 1), this particular combination shows the lowest stress relaxation and strain recovery values. Given that elevated temperature and humidity reduce both modulus and strain recovery, continuous folding can cause a non-uniform thickness of the sample due to adhesive deformation, especially when the adhesive already exhibits compromised strain recovery. Such non-uniformity ultimately leads to the formation of cracks during the folding test. Remarkably, the EHA:HBA combination remained crack-free under all conditions. This film, the EHA:HBA blend, nearly aligns with the benchmarks set for commercial OCA films in terms of adhesion, viscoelastic properties, and folding tests.

2.6. Demonstration

Finally, we carried out tests to assess the removal process of our UV-debondable OCA from UTG and CPI substrates. Recently,

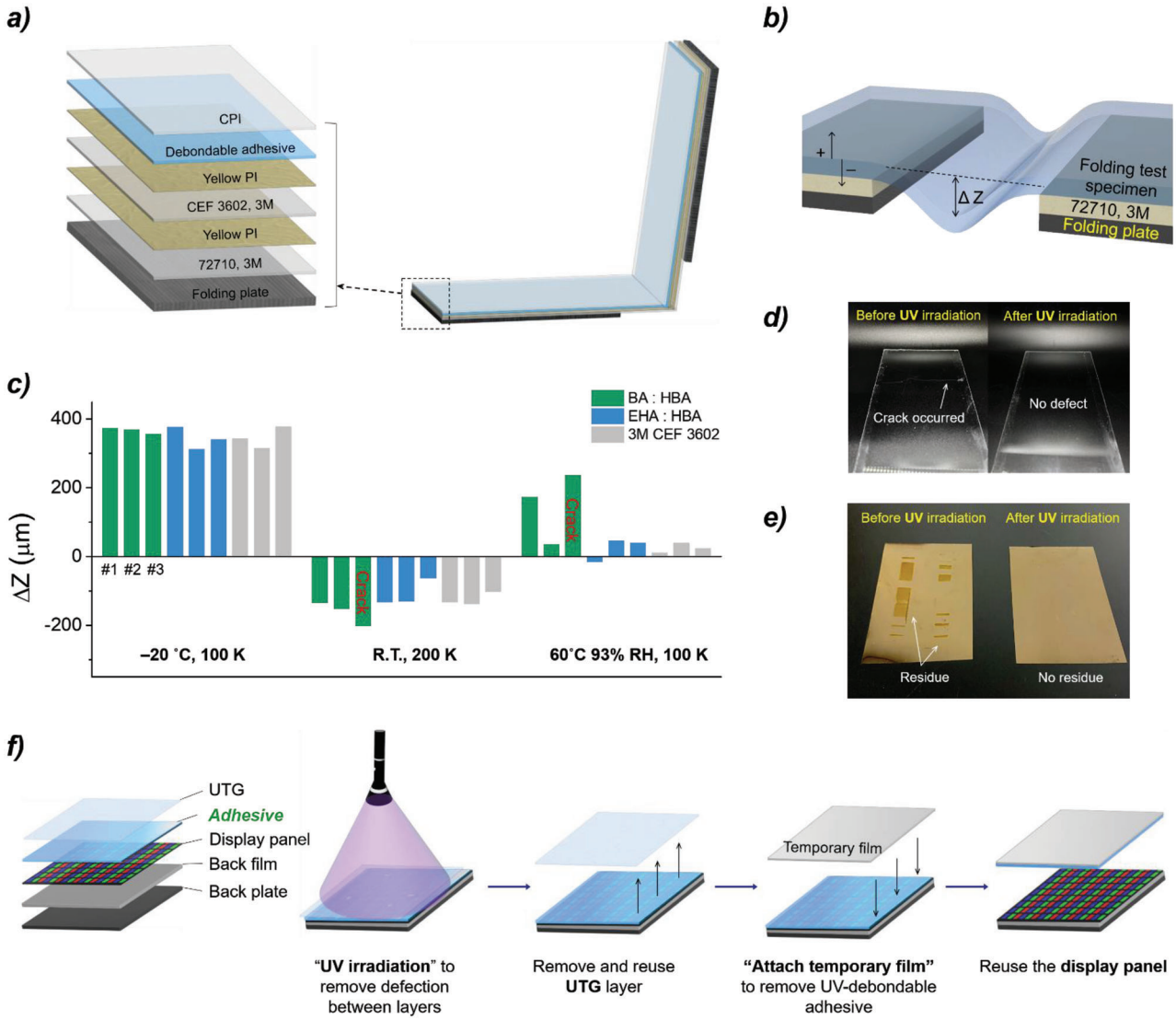

Figure 4. a) Structure of the folding test specimen, b) *Z*-axis displacement (ΔZ) was determined using surface profiling following the folding test, and c) ΔZ values were recorded for three samples from each of the entries; sample that cracked during the folding test were identified. d) High adhesion creates a robust bond between the adhesive and UTG, potentially leading to cracks during the debonding process. In contrast, the reduced adhesion observed after UV irradiation allows for easier peeling from UTG, minimizing the likelihood of defect formation. e) Strong bonding between PI and adhesive leaves residues on the surface, while reduced adhesion due to curing results in a clean substrate without any residue. f) Proposed process for layer reusability using UV-debondable adhesive. This method allows for the complete separation of UTG and the display panel without leaving any residues, utilizing only UV light and a temporary adhesive film.

there has been a rising demand for an effective solution to address air bubbles or misalignment defects between layers in the display manufacturing process. This is driven by the goal of enhancing the reusability of expensive UTG and display panel components. When trying to separate UTG from OCA with a view to reuse the layers, the inherent brittleness of UTG makes it susceptible to the adhesive strength of the OCA, often resulting in cracks (Figure 4d). Consequently, the current method of reuse entails the use of thermal energy to weaken and detach the OCA bonding between the UTG and the display panel. After the layers are separated, their surfaces undergo chemical treatment and surface wiping to eliminate any OCA residue before reuse (Figure S22, Supporting Information). The reusability of the UTG layer stands as a critical factor in large-scale display manufacturing, especially since production costs escalate notably as display size grows.[52] Hence, there is clear potential for significant cost savings if the layers can be reused by solely removing the OCA from both the UTG and the display panel, all the while ensuring defect-free results.

Figure 4f presents a simplified and effective separation process made possible by the UV-debondable adhesive, thereby eliminating the need for thermal energy and chemical treatments. Introducing this UV-debondable adhesive between the UTG and display panel, and then subjecting it to UV irradiation, allows for the residue-free removal of the UTG due to the reduced peel strength. Our experiments involving the removal of

UV-irradiated debondable adhesive from UTG confirmed a dramatic reduction in the adhesion between the UTG and OCA, ensuring flawless delamination. Any adhesive film left on the panel after UV irradiation can be easily removed with a temporary adhesive. For instance, when a temporary film, such as conventional Scotch tape, adheres to the debondable adhesive, it facilitates both simultaneous detachment and subsequent removal from the display panel. On the other hand, for OCAs without UV-debonding capability, a significant amount of residue remained after removal from UTG or CPI (Figure 4e); this phenomenon suggests that UV irradiation causes the OCA to transition its fracture mode from cohesive to adhesive failure, thereby corroborating the findings from earlier rheology tests (Figure 2e) and simulations (Figure 3). Notably, during the separation from UTG, there were instances where the UTG either shattered or numerous micro-cracks appeared on its surface. Nevertheless, this approach simplifies the processes compared to existing methods, requiring only a light source for layer separation, and thereby facilitating component reuse should defects arise during manufacturing.

3. Conclusion

In conclusion, our work introduces an innovative OCA custom-tailored for foldable displays. This adhesive not only meets the essential requirements for its application in foldable devices but also possesses a unique feature: selective removal through UV irradiation. By incorporating benzophenone derivatives into the polymer network, we achieved rapid and on-demand debonding. This integration promotes additional crosslinking via UV-induced Norrish type II reactions, effectively facilitating debonding at the adhesive-substrate interface. A significant highlight of our approach is the utilization of visible-light-driven radical polymerization to engineer the OCA films. This technique offers outstanding compatibility with various monomers and orthogonal reactivity with benzophenone, making it exceptionally well-suited for large-scale production. The resulting OCA film exhibits remarkable performance, especially with the formulation of a precise blend of acrylic monomers and 3 mol% of benzophenone-derived acrylates. This formulation substantially reduces adhesion, allowing effortless removal of the adhesive from UTG and display panels without leaving residue. Additionally, the prepared OCA film showcases remarkable attributes, including high optical transparency (99%) and robust peel strength (2.76 N cm^{-1}), along with balanced stress relaxation and strain recovery. Its superior folding durability is evident, remaining defect-free even after rigorous dynamic folding tests. These outcomes align closely with the strict specifications required for commercial foldable displays. The contributions presented in this study pave the way for the development of advanced adhesives with controlled removal capabilities, addressing the needs of emergent technologies like foldable displays and micro LED transfer. The strategic blend and incorporation of UV-responsive elements present a promising solution for enhancing manufacturing efficiency and product reliability in the upcoming electronics/displays industry and the sustainable plastics industries.

Supporting Information

Supporting Information is available from the Wiley Online Library or from the author.

Acknowledgements

D.K. designed the experiments, analyzed the data, and prepared the manuscript. H.K. performed molecular dynamic simulations and analyzed the data. D.K. and H.K. equally contributed to the work. The work from SNU was supported by the Technology Innovation Program (20011317, Development of an adhesive material capable of morphing more than 50% for flexible devices with a radius of curvature of 1 mm or less) funded by the Ministry of Trade, Industry & Energy (MOTIE, Korea). It was also backed by the National Research Foundation of Korea (NRF) grants provided by the Ministry of Science and ICT (MSIT, Korea) under grant numbers 2021R1A5A1030054 and 2022R1A2C2011627, and by LG Display through the LGD-SNU Incubation Program. The work from HYU was supported by the NRF grant funded by the MSIT (No. RS-2023-00210865).

Conflict of Interest

The authors declare no conflict of interest.

Data Availability Statement

The data that support the findings of this study are available in the supplementary material of this article.

Keywords

debondable adhesive, reworkable adhesive, sustainable adhesive, switchable adhesive, visible-light curing

Received: September 23, 2023
Revised: December 19, 2023
Published online: January 3, 2024

[1] T. Elmqvist, E. Andersson, N. Frantzeskaki, T. Mcphearson, P. Olsson, O. Gaffney, K. Takeuchi, C. Folke, *Nat. Sustainability* **2019**, *2*, 267.
[2] G. Harper, R. Sommerville, E. Kendrick, L. Driscoll, P. Slater, R. Stolkin, A. Walton, P. Christensen, O. Heidrich, S. Lambert, A. Abbott, K. Ryder, L. Gaines, P. Anderson, *Nature* **2019**, *575*, 75.
[3] S. Saito, S. Nobusue, E. Tsuzaka, C. Yuan, C. Mori, M. Hara, T. Seki, C. Camacho, S. Irle, S. Yamaguchi, *Nat. Commun.* **2016**, *7*, 12094.
[4] T. Ohzono, M. O. Saed, E. M. Terentjev, *Adv. Mater.* **2019**, *31*, 1902642.
[5] G. D. Crevoisier, P. Fabre, J.-M. Corpart, L. Leibler, *Science* **1999**, *285*, 1246.
[6] S. Salimi, T. S. Babra, G. S. Dines, S. W. Baskerville, W. Hayes, B. W. Greenland, *Eur. Polym. J.* **2019**, *121*, 109264.
[7] S. Leijonmarck, A. Cornell, C.-O. Danielsson, T. Åkermark, B. D. Brandner, G. Lindbergh, *Int. J. Adhes. Adhes.* **2012**, *32*, 39.
[8] T. S. Babra, A. Trivedi, C. N. Warriner, N. Bazin, D. Castiglione, C. Sivour, W. Hayes, B. W. Greenland, *Polym. Chem.* **2017**, *8*, 7207.
[9] T. Oguri, A. Kawahara, N. Kihara, *Polymer* **2016**, *99*, 83.
[10] R. La Spina, M. R. Tomlinson, L. Ruiz-Pérez, A. Chiche, S. Langridge, M. Geoghegan, *Angew. Chem., Int. Ed.* **2007**, *46*, 6460.
[11] T. Nakamura, Y. Takashima, A. Hashidzume, H. Yamaguchi, A. Harada, *Nat. Commun.* **2014**, *5*, 4622.

[12] Y. Gao, K. Wu, Z. Suo, *Adv. Mater.* **2018**, *31*, 1806948.
[13] H. Akiyama, M. Yoshida, *Adv. Mater.* **2012**, *24*, 2353.
[14] R. D. Adams, *Adhesive Bonding: Science, Technology and Applications*, Woodhead Publishing, Oxford, **2021**.
[15] Y. Lu, J. Broughton, P. Winfield, *Int. J. Adhes. Adhes.* **2014**, *50*, 119.
[16] H.-W. Chen, J.-H. Lee, B.-Y. Lin, S. Chen, S.-T. Wu, *Light: Sci. Appl.* **2018**, *7*, 17168.
[17] S. Rose, A. Prevoteau, P. Elzière, D. Hourdet, A. Marcellan, L. Leibler, *Nature* **2014**, *505*, 382.
[18] Z. Bai, Y. Xu, C. Lee, J. Guo, *Adv. Funct. Mater.* **2021**, *31*, 2104365.
[19] Y. Li, C. P. Wong, *Mater. Sci. Eng., R* **2006**, *51*, 1.
[20] J. H. Back, Y. Kwon, H. Cho, H. Lee, D. Ahn, H. J. Kim, Y. Yu, Y. Kim, W. Lee, M. S. Kwon, *Adv. Mater.* **2023**, *35*, 2204776.
[21] Ultra-thin Glass Market: Global Industry Trends, Share, Size, Growth, Opportunity and Forecast 2023–2028, IMARC Services Pvt. Ltd. **2023**.
[22] J. C. Scaiano, E. B. Abuin, L. C. Stewart, *J. Am. Chem. Soc.* **1982**, *104*, 5673.
[23] K. R. Mulcahy, A. F. R. Kilpatrick, G. D. J. Harper, A. Walton, A. P. Abbott, *Green Chem.* **2022**, *24*, 36.
[24] C. Guo, Z. Pan, C. Li, S. Zou, C. Pang, J. Wang, J. Hu, Z. Gong, *npj Flexible Electron.* **2022**, *6*, 44.
[25] C. Bandl, W. Kern, S. Schlögl, *Int. J. Adhes. Adhes.* **2020**, *99*, 102585.
[26] C. Hwang, J.-H. Back, D. Ahn, H.-J. Paik, W. Lee, Y. Yu, *Polym. Chem.* **2022**, *13*, 193.
[27] A. Al Mousawi, D. M. Lara, G. Noirbent, F. Dumur, J. Toufaily, T. Hamieh, T.-T. Bui, F. Goubard, B. Graff, D. Gigmes, J. P. Fouassier, J. Lalevée, *Macromolecules* **2017**, *50*, 4913.
[28] M. Abdallah, H. Le, A. Hijazi, M. Schmitt, B. Graff, F. Dumur, T.-T. Bui, F. Goubard, J.-P. Fouassier, J. Lalevée, *Polymer* **2018**, *159*, 47.
[29] P. Wen, Y. Zhao, Z. Wang, J. Lin, M. Chen, X. Lin, *ACS Appl. Mater. Interfaces* **2021**, *13*, 8426.
[30] J. C. Theriot, C.-H. Lim, H. Yang, M. D. Ryan, C. B. Musgrave, G. M. Miyake, *Science* **2016**, *352*, 1082.
[31] J. Xu, K. Jung, A. Atme, S. Shanmugam, C. Boyer, *J. Am. Chem. Soc.* **2014**, *136*, 5508.
[32] N. Corrigan, J. Yeow, P. Judzewitsch, J. Xu, C. Boyer, *Angew. Chem., Int. Ed.* **2019**, *58*, 5170.
[33] C. Dietlin, S. Schweizer, P. Xiao, J. Zhang, F. Morlet-Savary, B. Graff, J.-P. Fouassier, J. Lalevée, *Polym. Chem.* **2015**, *6*, 3895.
[34] P. Xiao, J. Zhang, F. Dumur, M. A. Tehfe, F. Morlet-Savary, B. Graff, D. Gigmes, J. P. Fouassier, J. Lalevée, *Prog. Polym. Sci.* **2015**, *41*, 32.
[35] M. A. Tasdelen, J. Lalevée, Y. Yagci, *Polym. Chem.* **2020**, *11*, 1111.
[36] Y. Kwon, J. Lee, Y. Noh, D. Kim, Y. Lee, C. Yu, J. C. Roldao, S. Feng, J. Gierschner, R. Wannemacher, M. S. Kwon, *Nat. Commun.* **2023**, *14*, 92.
[37] Y. Lee, M. S. Kwon, *Eur. J. Org. Chem.* **2020**, *38*, 6028.
[38] V. K. Singh, C. Yu, S. Badgujar, Y. Kim, Y. Kwon, D. Kim, J. Lee, T. Akhter, G. Thangavel, L. S. Park, J. Lee, P. C. Nandajan, R. Wannemacher, B. Milián-Medina, L. Lüer, K. S. Kim, J. Gierschner, M. S. Kwon, *Nat. Catal.* **2018**, *1*, 794.
[39] Y. Kwon, S. Lee, J. Kim, J. Jun, W. Jeon, Y. Park, H.-J. Kim, J. Gierschner, Y. Kim, M. S. Kwon, *Nat. Commun.* https://doi.org/10.21203/rs.3.rs-3313870/v1.
[40] G. Dormán, H. Nakamura, A. Pulsipher, G. D. Prestwich, *Chem. Rev.* **2016**, *116*, 15284.
[41] S. K. Christensen, M. C. Chiappelli, R. C. Hayward, *Macromolecules* **2012**, *45*, 5237.
[42] Z. Czech, A. Kowalczyk, J. Kabatc, J. Swiderska, *Eur. Polym. J.* **2012**, *48*, 1446.
[43] Z. Czech, *Eur. Polym. J.* **2004**, *40*, 2221.
[44] C.-H. Park, S.-J. Lee, T.-H. Lee, H.-J. Kim, *Int. J. Adhes. Adhes.* **2015**, *63*, 137.
[45] Z. Czech, M. Wesolowska, *Eur. Polym. J.* **2007**, *43*, 3604.
[46] J. Chilton, L. Giering, C. Steel, *J. Am. Chem. Soc.* **1975**, *98*, 1865.
[47] S. Zhu, A. Das, L. Bui, H. Zhou, D. P. Curran, M. Rueping, *J. Am. Chem. Soc.* **2013**, *135*, 1823.
[48] J. W. Beatty, C. R. J. Stephenson, *Acc. Chem. Res.* **2015**, *48*, 1474.
[49] S.-K. Kwon, J.-H. Baek, H.-C. Choi, S. K. Kim, R. Lampande, R. Pode, J. H. Kwon, *RSC Adv.* **2019**, *9*, 42561.
[50] S. Sun, M. Li, A. Liu, *Int. J. Adhes. Adhes.* **2013**, *41*, 98.
[51] C. J. Campbell, J. Clapper, R. E. Behling, B. Erdogan, H. Z. Beagi, J. T. Abrahamson, A. I. Everaerts, *SID Int. Symp. Dig. Tech. Pap.* **2017**, *48*, 2009.
[52] A. Plichta, A. Habeck, S. Knoche, A. Weber, N. Hildebrand, in *Flexible Flat Panel Displays*, (Ed.: G. P. Crawford), John Wiley & Sons, **2005**, p. 35.